File
039-153

(6) LASER MEANS OF SYNTHESIZING AND MODIFYING REFRACTORY POWDERS.

AD A068628

B.S.

(10) Principal Investigators:

Dr. John S. Haggerty 617-253-2129
Dr. W. Roger Cannon 617-253-6472

Contractor:

Massachusetts Institute of Technology
77 Massachusetts Avenue
Cambridge, MA 02139

(11) 31 May 78

(12) 22 p.

ARPA Order No. 3449
Program Code No.: NR039-153
Contract No.: (15) N00014-77-C-0581, ARPA Order - 3449
Contract Date: 1 July 1977
Contract Expiration Date: 30 June 1979
Contract Amount $256,580.00
(9) Status Report, Period: 1 Feb. - 31 March 1978, No. 2,

220 000

Introduction

The object of research performed under this contract is to use a laser beam to synthesize and/or modify ceramic powders to obtain powders of very high quality for use in sintering or hot pressing. Among the powder qualities known to be highly desireable for sintering are small diameter, narrow size distribution, impurity control and a nearly spherical shape. The laser offers a clean heat source without a hot-walled chamber, and a well defined and controlled hot zone.

Initially, synthesis and modification of silicon nitride is being investigated. Three techniques are being developed:
(1) Size reduction and property modification of powders. (2) Synthesis of fine uniformly-sized powders formed from gas phase reactants. (3) Synthesis of composite particles formed by pyrolysing a gas phase reactant onto the surface of a heated particle.

Status

This is the second of the reports issued on a bi-monthly basis to bring the schedule onto a July, September, December, March report scheme. The next report in July, will be the annual report.

During this report period, work has progressed on techniques (1) and (2) above, while technique (3) will await development this next year. Under technique (1), powder modification, the following results were obtained:
(a) Air entrained particles were successfully passed thro gh the waist of the laser beam at a flow rate near the Stokes settling velocity and recovered.
(b) Static experiments were continued and it was determined that the technique is limited by laser power.

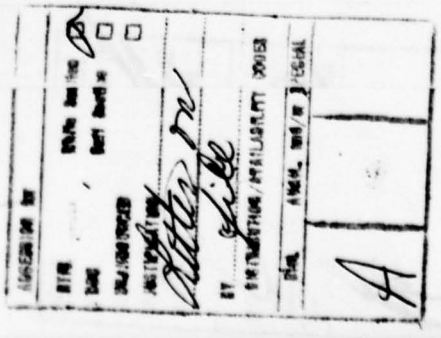

(c) Comminution models were further studied and evidence for both $N_2(g)$ evolution alone and $N_2(g)$ + Si(g) evolution were found.

In the portion of the program directed toward synthesizing silicon nitride powders from silane and ammonia, the following results were obtained: (a) The absorption coefficient of ammonia was measured and (b) powders were synthesized from a equimolar mixture of silane and ammonia. They were found to be very uniformly sized.

As of April 1, John Flint and Professor Forbes Dewey of the Mechanical Engineering Department will be supported part-time under this contract. Previously they were contributing, but under funds from the M.I.T. Energy Laboratory. Steven Danforth recently graduated from Brown University with a Ph.D. and has joined the program on a full-time basis as a postdoctoral student.

Powder Size and Shape Modification

As we reported previously, while particle comminution was achieved by passing particles through nearly focused CO_2 laser beams, the extent and rate of diameter reduction were not as high as our calculations had predicted. These flight experiments were not carried out under conditions where power intensity and exposure time were maximized. For these reasons, during this period, we have concentrated on maximizing the exposure to which the particles are subjected in flight experiments, as well as continuing to map out the experimental conditions which result in diameter reduction with the static-pulsed experiments reported previously.

Near the focal length, the radius of light beam differs substantially from a simple linear convergence to a point which is a good approximation

at other locations along the beam axis. The exact description depends on a number of factors including the energy and wavelength distributions in the emitted light beam. Dickson[1] has analyzed the $1/e^2$ radius of a propagating gaussian beam as a function of initial radius and lens focal length. The results of these calculations applied to the CO_2 laser and 5 inch nominal focal length lens used in these experiments are given in Figs. 1 and 2. Fig. 1 shows experimentally measured "burn spot" radii as well as the calculated beam radius as a function of distance from the lens. Fig. 2 is an expansion of the region near the focal length. The power densities are calculated on the basis of a 170 watt maximum emitted CW power. The peak power in the pulsed mode is approximately 5-10 times higher than the maximum CW power level. The maximum power density which we can achieve with the available equipment in its present configuration is approximately 2×10^5 watts/cm^2 in a CW mode and in excess of 10^6 watts/cm^2 in a pulsed mode. Modifying the equipment to use a 2 1/2 inch focal length lens will reduce the minimum bean radius by approximately a factor of two, giving powder densities which are four times higher; however, injecting the particles into the center of a 180 μm diameter region presents a difficult problem.

The power balance between the heat absorbed and the various heat loss mechanisms has been examined further. This equality is:

$$I \frac{\pi d^2}{4} Q_{abs} = C_p \frac{\pi d^3}{6} \rho \frac{dT}{dt} + h\pi d^2 (T - T_{amb}) + \varepsilon\sigma\pi d^2 (T^4 - T_{amb}^4) + J\pi d^2 \Delta H$$

where

I = beam intensity

d = particle diameter

Q_{abs} = Mie absorption efficiency

C_p = specific heat

ρ = density

h = convective heat transfer coefficient

ε = emissivity

σ = Boltzman radiation constant

J = specific molar vaporization rate

ΔH = molar heat of vaporization

For power densities greater than 10^3 watts/cm^2, the sensible heat term dominates the heat losses for temperatures up to levels where Si_3N_4 decomposes ($T \simeq 1900°C$). For power densities in the range of 10^4 watts/cm^2, heating rates of 40 μm diameter particles will be approximately 8×10^5°C/sec. Once temperatures are reached where an endothermic decomposition reaction proceeds, the last term in the expression dominates the heat losses and a nominally constant temperature reaction will proceed at a rate which is controlled by the power absorbed by the particle. The time-temperature history experienced by a particle can be approximated accurately by linear temperature rise to the decomposition temperature followed by a constant temperature plateau which persists until the absorption efficiency (Q_{abs}) decreases, because the particles become too small to couple efficiently. Fig. 3 shows predicted time-temperature curves for 40 μm diameter Si_3N_4 particles exposed to various power densities of 10.6 μm light. The $h = 0$ curve represents particles heated in vacuum to eliminate convective losses and $h = 29$ cal/sec·cm^2°K is a convective heat loss coefficient typical of a turbulent boundary layer in 1 atmosphere pressure air. For power densities greater than 5×10^3

watts/cm^2, convective loss mechanisms have a negligible effect on heating rate; however, ambient pressure might well be expected to effect vaporization kinetics. These results show that Si_3N_4 decomposition temperatures should be reached in a milisecond or less with power densities which are readily achieved with the laser which is being used.

Two decomposition mechanisms have been considered. In the first, which is typical of normal vaporization kinetics, Si_3N_4 decomposition to Si liquid and N_2(g): the heat for this decomposition reaction is 8.6×10^5 joules/mole. We have postulated that at higher vaporization rates, stoichiometric vaporization to Si gas and N_2 gas will occur with heat of sublimation of 2.0×10^6 joules/mole. The first reaction will leave a Si particle if the reaction proceeds to completion, which has a diameter equal of 94% of the diameter of the original 100% dense Si_3N_4 particle. Partial decomposition will produce a Si skin on a Si_3N_4 core. The sublimation reaction will leave a reduced diameter Si_3N_4 particle. Table I summarizes, for various power intensities, the times required for a 30 μm diameter Si_3N_4 particle to reach 2000°K, the times required to decompose it to Si according to the first model and the times required to reduce its diameter from 30 to 20 μm according to the second model.

CALCULATED RESIDENCE TIMES

$$Si_3N_4(s) \rightarrow 3Si(l) + 2N_2(g)$$
$$\Delta H = 8.6 \times 10^5 \text{ Joules/mole}$$

$$Si_3N_4(s) \rightarrow 3Si(g) + 2N_2(g)$$
$$\Delta H = 2.0 \times 10^6 \text{ Joules/mole}$$

I(w/cm^2)	Transient time to 2000°K	Decomposition time	Sublimation time (30→20 μm)
10^3	20×10^{-3}	58.6×10^{-3}	110×10^{-3}
10^4	1.5×10^{-3}	5.86×10^{-3}	11×10^{-3}
10^5	0.2×10^{-3}	0.59×10^{-3}	1.1×10^{-3}

We recognize that these two model responses of the particles to the laser are both simplified and idealized. The particles may respond in a number of possible ways which involve different diameter reduction mechanisms and rate controlling processes. For instance, nonisotropic vaporization can self-propel the particles out of the assumed trajectory at near sonic velocities. The vaporization products may shield the particles from the incident radiation and either absorbed water, shockwaves or rapidly expanding N_2 gas could cause the particles to explosively eject debris by non-vaporization processes. The two models analyzed in Table I, represent cases where heat input is rate limiting.

Fig. 4 summarizes experimental conditions under which diameter reduction has been achieved, operational limits which are accessible with the existing equipment and predicted times required to reduce particle diameters. In static experiments, Si_3N_4 particles were placed on Si substrates and subjected to varying intensity and duration pulses. The irradiated regions were examined microscopically to determine the conditions which resulted in particle size reduction. These conditions are grouped into three catagories: no size reduction, size reduction less than 50% of non-irradiated diameter, size reduction greater than 50% of non-irradiated diameter. The combinations of power intensity and pulse length which resulted in diameter reduction are demarked by the cross-hatched region on the figure. The dotted line captioned "Maximum CW Power" represents the maximum power density which can be achieved with the existing laser (P_{max} = 170 watts CW) and focusing optics (5 inch focal length lens). The 3 lines captioned "Stokes Settling Velocity" represent the time required for particles to pass through the laser spot of a diameter corresponding to the indicated power density with the laser operated at maximum CW power when the particles travel at their stoke's settling velocity. These curves represent the maximum exposure times which can be achieved

with various particle sizes since the actual particle velocity must exceed the settling velocity in most experimental configurations. Thus, the only set of conditions where comminution can be anticipated in flight experiments, based on the pulsed experiments, is the double cross-hatched, triangular region at power intensities ranging from approximately 1-2 x 10^5 watts/cm^2 and dwell times from 2-10 x 10^{-3} sec. The line captioned "Sublimation" represents the time calculated to reduce the diameter of Si_3N_4 nitride particles from 30 to 20 μm (the sum of the second and fourth columns in Table I). At a power density of 10^5 watts/cm^2 the agreement between the calculated dwell time and the pulse length of the static experiments is within a factor of 5 and appears to be improving at higher power densities. However, at lower intensities the agreement between calculated and experimental values is not good. We do not understand this discrepancy and the trend at this time. Most of the deviations from the assumed models should make the agreement better at lower power densities and worse at higher power densities in contrast to the observed behavior. One possible explanation is that at lower power densities and longer exposure times, the Si_3N_4 particles are partially decomposing to form a Si skin which decouples from the laser. Further analyses and continued particle characterization are underway to attempt resolving this fundamental issue.

The photomicrographs, Figs. 5, 6, and 7, show Si_3N_4 particles which have been subjected to the CO_2 laser beam. The central region of Fig. 5 is the area which was pulsed in a static experiment and it along with Fig. 6, illustrate that 20-30 μm diameter particles are reduced in diameter to 10-20 μm. The 8 μm diameter particle shown in Fig. 7 was caught on the filter after passing through the beam in a flight experiment. By the absence of a solidification morphology or texture, we conclude that there was very little, if any, liquid Si produced in these experiments. We also conclude by the

approximate equality between the number of particles per unit area of substrate in the irradiated and non-irradiated regions, as well as the size of the comminuted particles in relation to the uneffected particles, that the comminution process does not result from splitting or fracturing the particles into pieces which are major fractions of the original particle, i.e., they don't fracture into halves, thirds, or quarters, etc. This result suggests that these particles were reduced in diameter either by vaporization or by ejecting very small pieces of debris by an undefined mechanism. We are continuing to characterize the particles and debris, such as the 2 μm particles shown in Fig. 6, to confirm this observation.

Particles like those shown in Fig. 8 are produced in maximum power intensity flight experiments, but they were caught in a direction roughly parallel to the direction of the laser beam, rather than on the filter along the path of their injected trajectory. They were evidently self-propelled by nonisotropic vaporization. These particles were clearly liquid at some time based on their smooth spherical morphology, and have final diameters which are essentially equal to the original particles. Both characteristics are expected if the Si_3N_4 particles decompose to Si liquid and N_2 gas.

These results indicate that two distinct reaction mechanisms can result when Si_3N_4 particles are subjected to high intensity 10.6 μm radiation. It appears that they either decompose or sublime according to

$$Si_3N_4(s) \rightarrow 3Si(\ell) + 2N_2(g)$$

or

$$Si_3N_4(s) \rightarrow 3Si(g) + 2N_2(g)$$

depending on the power density and exposure time. Much careful work is required to confirm that these are the operating mechanisms and to identify

the conditions where each dominates. Both mechanisms can be used to advantage if adequately controlled. Controlled sublimation should result in uniform size, spherically shaped particles as we initially proposed. Partial decomposition of the Si_3N_4 particles should leave a Si skin on the Si_3N_4 cores which is the composite structure we desired to enhance reactive sintering. We will also attempt to form particles with this structure by pyrolizing a gaseous Si reactant onto laser heated Si_3N_4 particles.

Synthesis of Silicon Nitride from the Gas Phase

The previous bi-monthly report contained results on the measured absorption coefficient of silane to the wavelength output of our CO_2 laser, and reported the synthesis of silicon from silane using the laser as an energy source. The measured absorption coefficient for silane was between 8-10 cm^{-1} atm^{-1} depending on the radiation intensity.

During this report period, an absorption coefficient for ammonia was measured by the same technique. The measured value is 0.36 cm^{-1} atm^{-1}. This compares with a literature value[2] of 0.12 $cm^{-1}atm^{-1}$ for the P(20) line. These literature values, however, were obtained in from 10 to 357 ppm of ammonia in 1 atmosphere of air. Line broadening would account for the difference.

The results of these absorption measurements indicate that a silane-ammonia gas mixture will be heated by absorption of radiation preferentially by silane. However, provided collision frequency is of the order or less than the absorption frequency, both gases will heat thermally at the same rate. The mixture of 10:1 ammonia to silane will be an efficient absorber of energy according to the measured absorption coefficients. The mixture should absorb 91% of the beam in 1 cm at one atmosphere. This energy will be used very

efficiently when a gas stream the width of the laser beam is introduced into and normal to the beam.

This is a very encouraging result, since it means that essentially all the energy will be used directly in the chemical reaction. Since the reaction

$$3SiH_4 + 4NH_3 \rightarrow Si_3N_4 + 12H_2$$

is an exothermic reaction, the energy contributed by the laser will be used entirely to heat the gas to a reaction temperature. A CO_2 laser has typically a 10-15% overall efficiency. Thus the entire powder synthesis process would have a 10-15% efficiency, not equaled by many powder synthesizing processes.

During this report period a nearly equi-mixture of silane and ammonia (25 torr silane, 29 torr ammonia) was pyrolysized in a 15 watt beam to produce a fine powder. The fine powder was light brown in color, similar to the powder synthesized from silane only last report period. The infrared spectrum of the two are compared in Fig. 8. They contained the broad bands at 4.6, 9, and 11.5 μm. The 11.5 μm peak was relatively larger, and the 9 μm peak smaller in the powder synthesized from the silane-ammonia mixture. The 4.6 μm peak likely corresponds to Si-H band absoprtion and the 9 μm the Si-O band absoprtion. The 11.5 μm peak is associated either with the Si-N or Si-H absorption. Since introducing the ammonia as a reactant increased this absorption band height, it is likely that it is associated with Si-N. Evidently the silicon in the powder synthesized from SiH_4 is partially oxidized and probably nitrided as it is exposed to air, but there is considerable free silicon as evidenced by the short wavelength absorption.

The decrease in the silicon-oxygen peak by about 1/2 when an ammonia-silane mixture is used, indicates that a large number of Si-N bands are formed which do not easily oxidize. The sharp decrease in short wavelength absorption indicates considerable silicon nitride forms.

Powders were examined under TEM, SEM, and STEM. Particles were determined by selected area defraction in the STEM to be amorphous. The particle size of the silane-ammonia synthesized powders was 200-400 Å and spherical. The particle size of the powders synthesized from silane powder was less uniform and varied between 200-1000 Å. The uniformity of the particle size in the former case is very encouraging and tends to confirm our original contention that by using the well defined "hot" zone of a laser, uniform particles could be produced.

In the coming quarter, larger ammonia-silane ratios will be used to increase the nitrogen content of the particles. A flowing gas system is now being constructed so that larger amounts of powder can be produced and a minimal amount of powder will form on the entrance window. With larger amounts of powder, additional characterization techniques will be available, such as sputtering ion mass spectroscopy (SIMS), DSC and TGA. Laser chemistry experiments are scheduled to begin during the summer. A tunable CO_2 laser will be available with high intensity pulse capabilities. Experiments will be initiated to alter the chemistry of powders and understand the nucleation process.

References

1. L. D. Dickson, Appl. Optics, 9, 1854 (1970).

2. R. R. Patty, G. M. Russwurm, W. A. McClenny and D. R. Morgan, Appl. Optics, 13, 2850 (1974).

Figure 1.

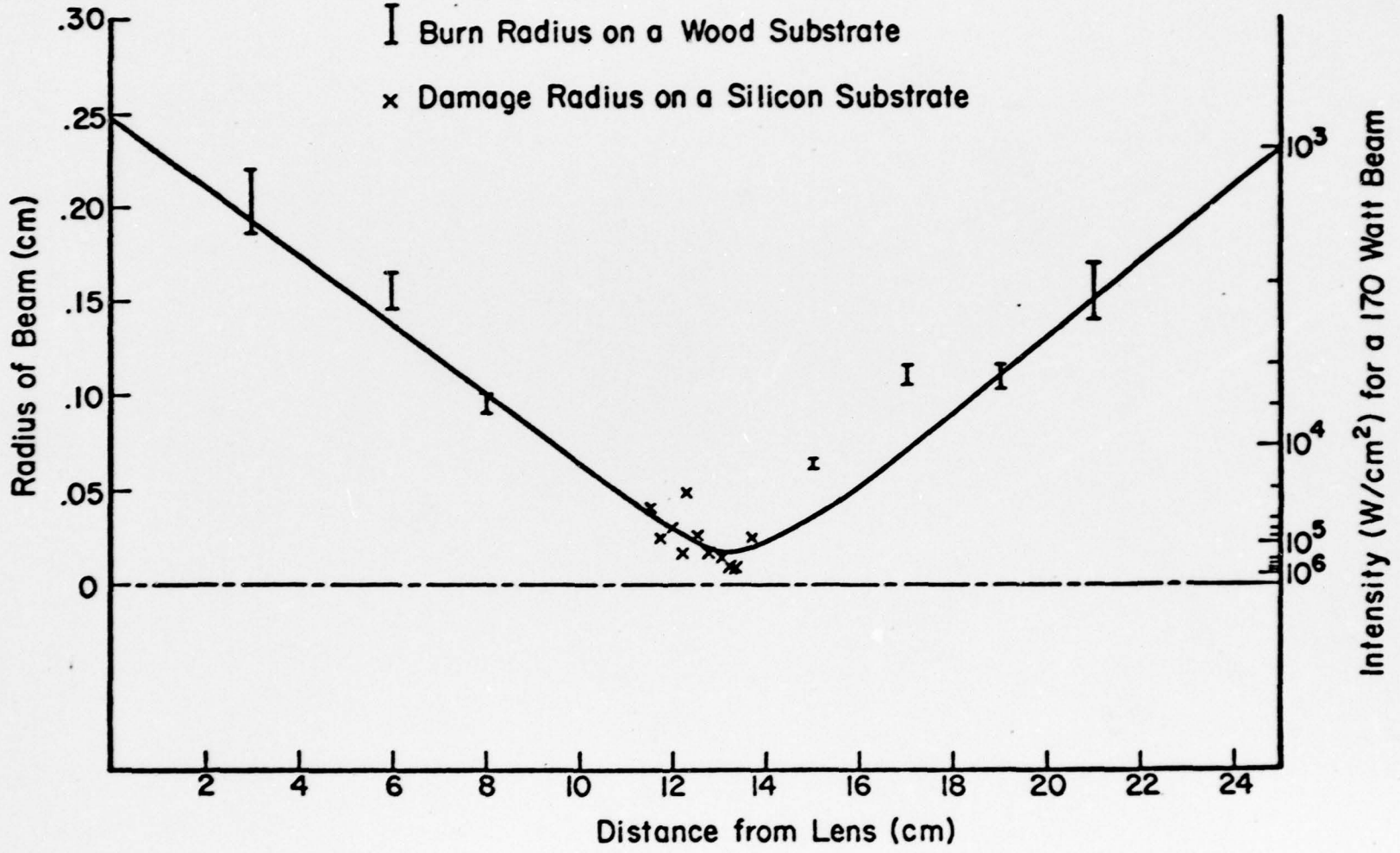

Figure 1. Beam radius to the $1/e^2$ intensity assuming a gaussian beam for our 13 cm focal length lens.

Figure 2.

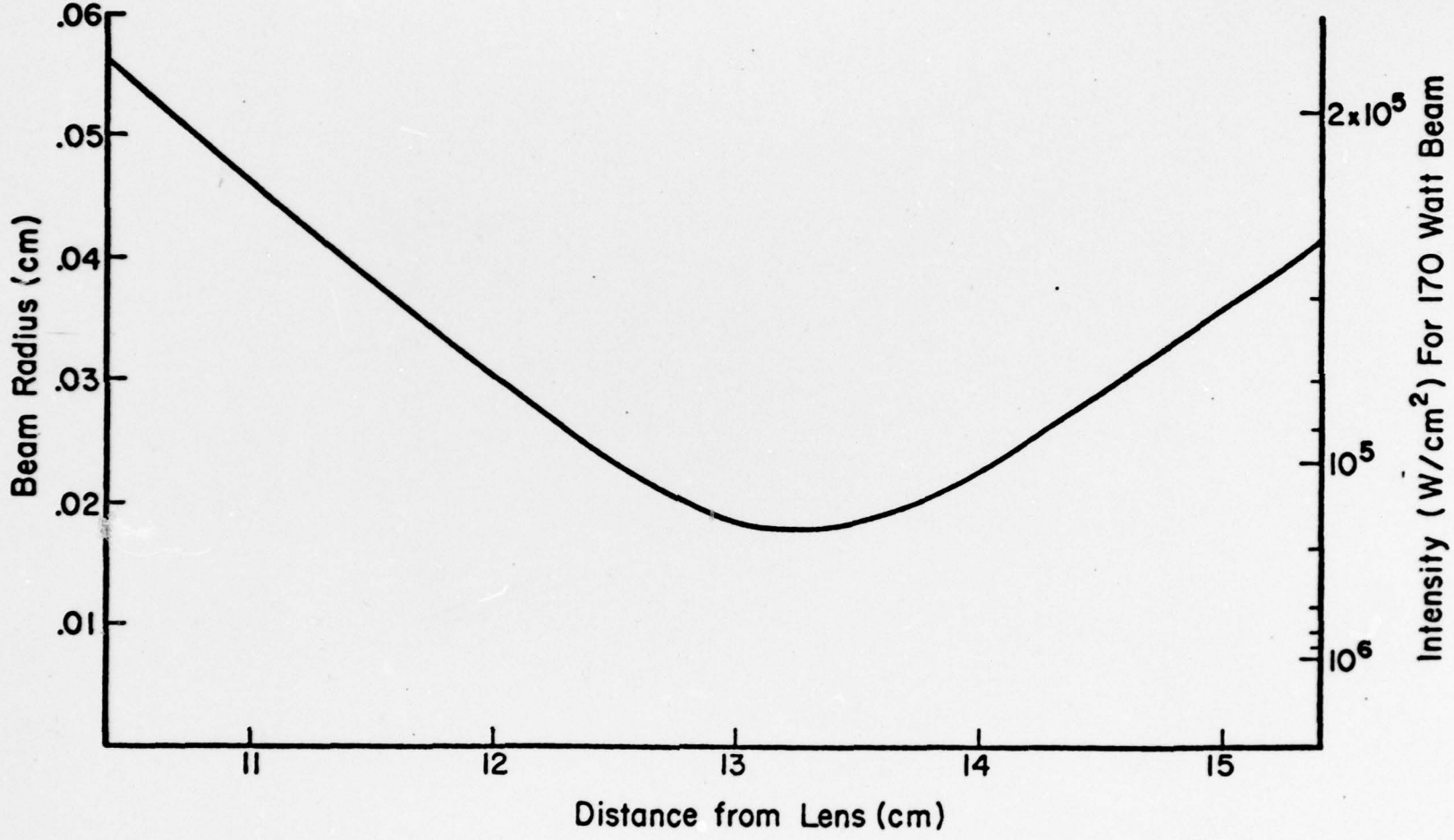

Figure 2. Same as Figure 1, but emphasizes the region near the focal point.

Figure 3.

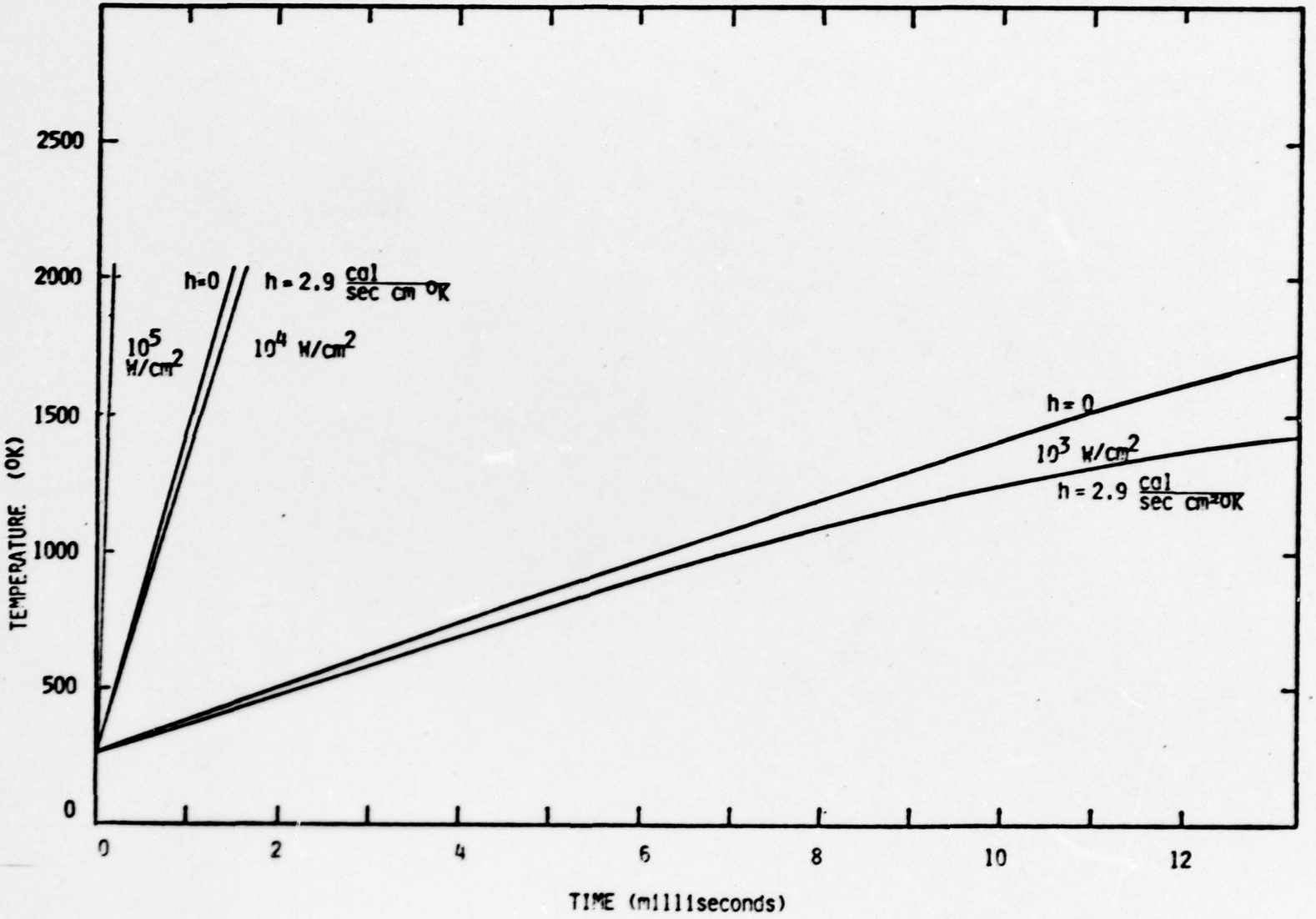

Figure 3. Particle temperature as a function of time of a 40 μm particle of silicon nitride irradiated at three different intensities. h is the heat transfer coefficient.

Figure 4.

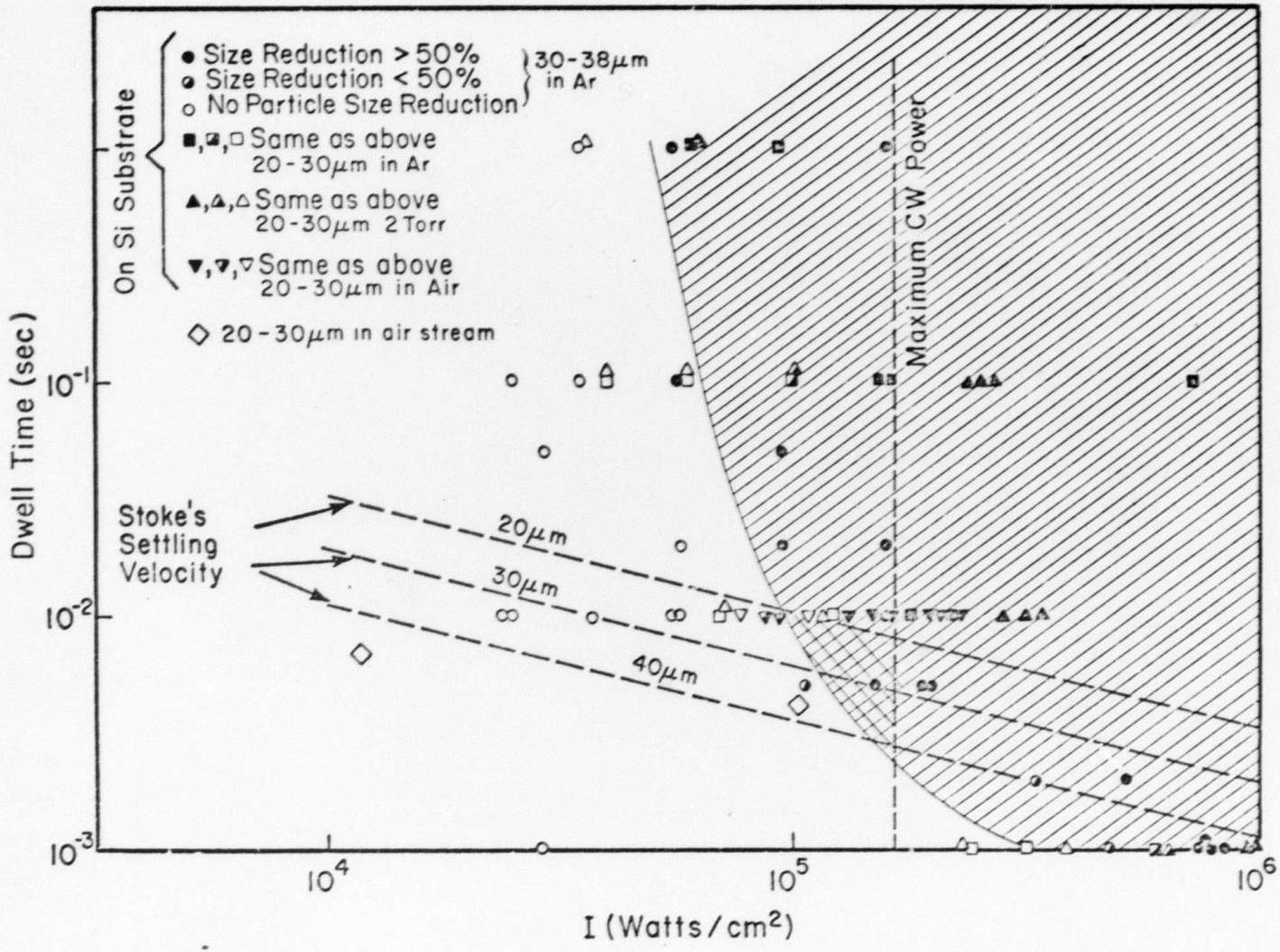

Figure 4. A map of the intensity and dwell times (pulse lengths) needed to reduce the particle size of silicon nitride powders spread over a silicon substrate or entrained in an air stream. The Maximum CW power refers to our laser's maximum power, 170 watts, and a 13 cm lens. The Stoke's Settling Velocity curves are explained in the text.

Figure 5.

Figure 5. A typical area of the static pulse experiment. In the center of the area particles are reduced in size by the laser pulse. 10 msec pulse $\sim$ 2 x 10^5 watts/cm^2.

Figure 6.

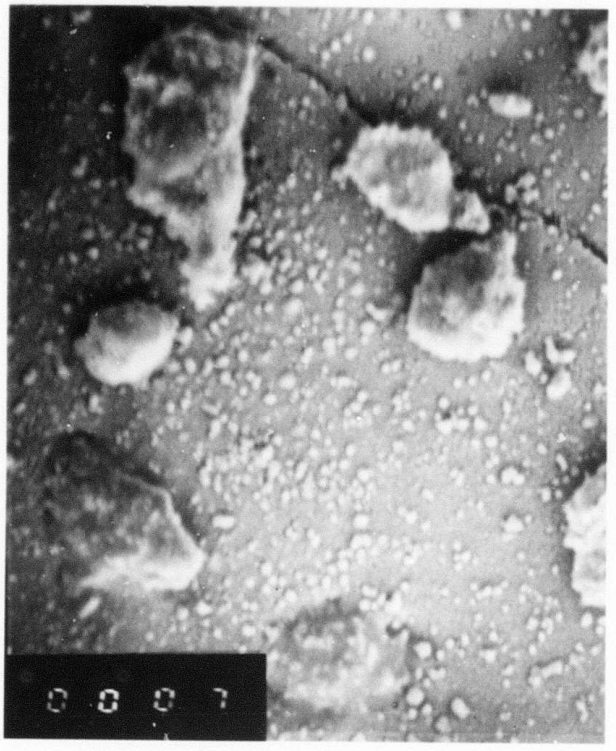

Figure 6. A close-up micrograph of a few of the particles at the center of the irradiated area shown in Fig. 5.

Figure 7.

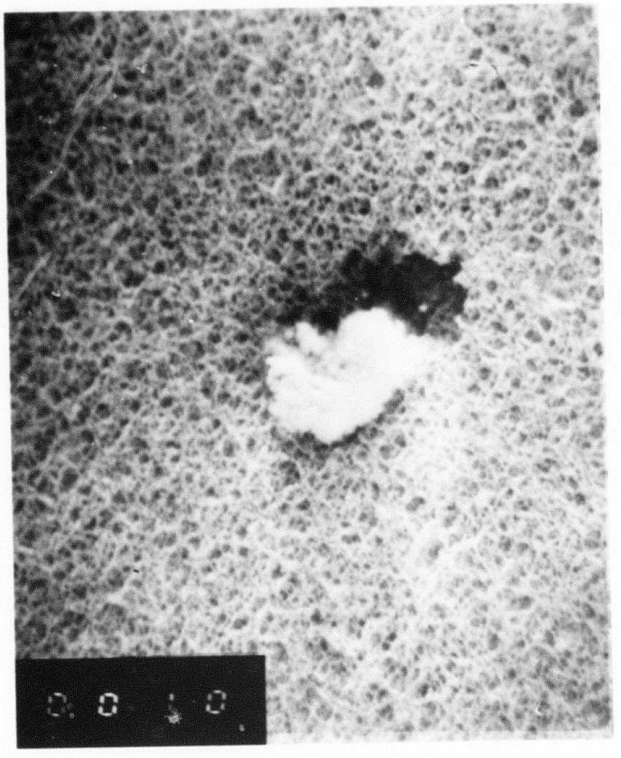

Figure 7. A particle caught on the filter during the particle flight experiment

Figure 8

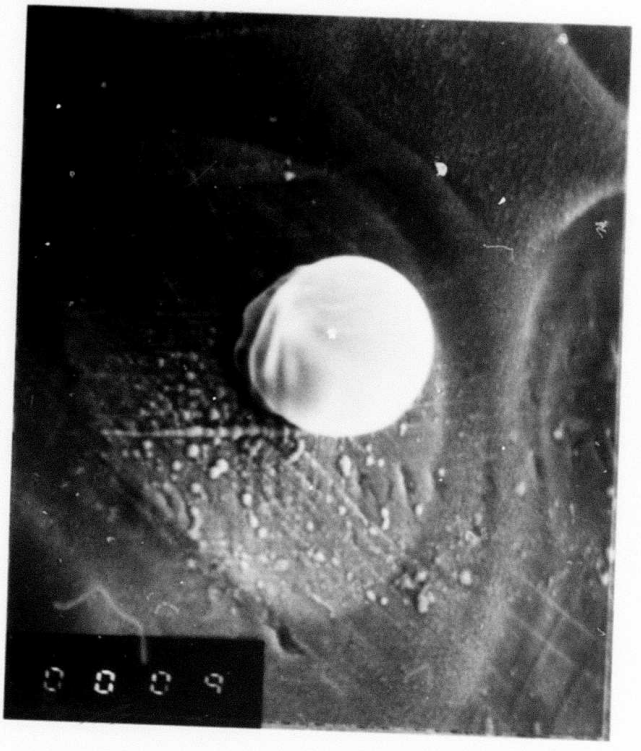

Figure 8. A particle caught near the axis of the beam during a particle flight experiment.

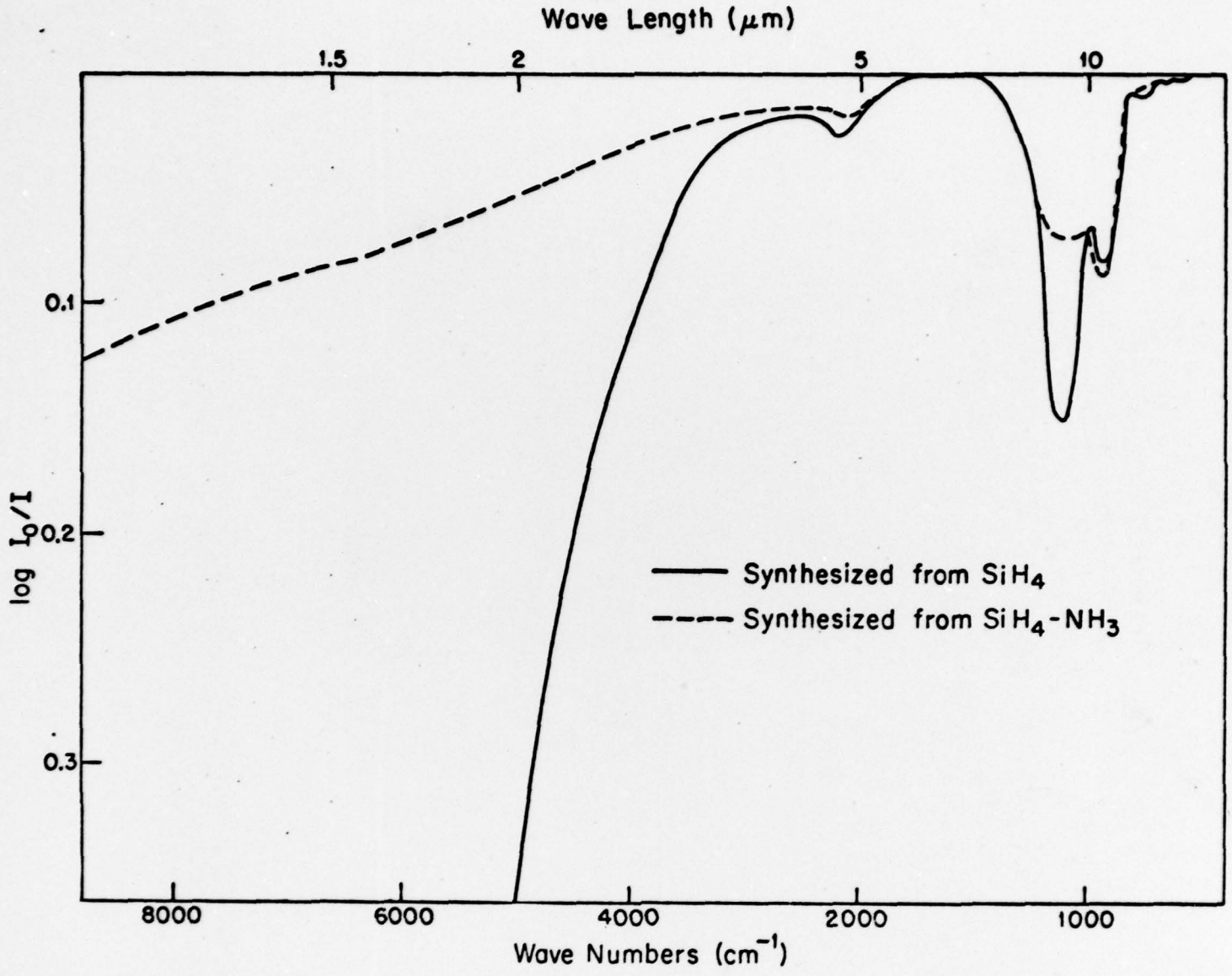

Figure 9. The infrared absorption spectra of power prepared from silane alone, and equi-molar mixture of silane plus ammonia.